



HAL
open science

The expanding LARS2 phenotypic spectrum: HLASA, Perrault syndrome with leukodystrophy, and mitochondrial myopathy

Lisa Riley, Joëlle Rudinger-thirion, Magali Frugier, Meredith Wilson, Melissa Luig, Thushari Indika Alahakoon, Cheng Yee Nixon, Edwin Kirk, Tony Roscioli, Sebastian Lunke, et al.

► To cite this version:

Lisa Riley, Joëlle Rudinger-thirion, Magali Frugier, Meredith Wilson, Melissa Luig, et al.. The expanding LARS2 phenotypic spectrum: HLASA, Perrault syndrome with leukodystrophy, and mitochondrial myopathy. *Human Mutation*, 2020, 41 (8), pp.1425-1434. 10.1002/humu.24050 . hal-02966089

HAL Id: hal-02966089

<https://hal.science/hal-02966089>

Submitted on 5 Nov 2020

HAL is a multi-disciplinary open access archive for the deposit and dissemination of scientific research documents, whether they are published or not. The documents may come from teaching and research institutions in France or abroad, or from public or private research centers.

L'archive ouverte pluridisciplinaire **HAL**, est destinée au dépôt et à la diffusion de documents scientifiques de niveau recherche, publiés ou non, émanant des établissements d'enseignement et de recherche français ou étrangers, des laboratoires publics ou privés.

The expanding *LARS2* phenotypic spectrum: HLASA, Perrault syndrome with leukodystrophy, and mitochondrial myopathy

Lisa G. Riley ^{1,2}, Joëlle Rudinger-Thirion ³, Magali Frugier ³, Meredith Wilson ^{4,5}, Melissa Luig ⁶, Thushari Indika Alahakoon ⁷, Cheng Yee Nixon ^{8,9}, Edwin P Kirk ^{9,10}, Tony Roscioli ¹⁰, Sebastian Lunke ^{11,12,13}, Zornitza Stark ^{11,13,14}, Klaas J. Wierenga ^{15,16}, Sirish Palle ¹⁵, Maie Walsh ¹⁷, Emily Higgs¹⁷, Susan Arbuckle ¹⁸, Shalini Thirukeswaran ^{14,19}, Alison G. Compton ^{14,19}, David R. Thorburn ^{11,14,19}, John Christodoulou ^{2,11,13,14,19}

¹Rare Diseases Functional Genomics, Kids Research, The Children's Hospital at Westmead and The Children's Medical Research Institute, Sydney, Australia

²Discipline of Child & Adolescent Health, Sydney Medical School, and ⁵Discipline of Genomic Medicine, University of Sydney, Sydney, Australia

³Université de Strasbourg, Architecture et Réactivité de l'ARN, CNRS, IBMC, Strasbourg, France

⁴Department of Clinical Genetics, The Children's Hospital at Westmead and ¹⁸Department of Pathology, The Children's Hospital at Westmead, Sydney, Australia

⁶Dept of Neonatology, Westmead Hospital, Sydney, Australia

⁷Westmead Institute for Maternal & Fetal Medicine, Westmead Hospital & University of Sydney, Australia

⁸Neuroscience Research Australia (NeuRA), University of New South Wales, Sydney, Australia

⁹Genetics Laboratory, NSW Health Pathology East and ¹⁰Centre for Clinical Genetics, Sydney Children's Hospital, Randwick, Sydney, Australia

¹¹Victorian Clinical Genetics Services and ¹⁹Murdoch Children's Research Institute, The Royal Children's Hospital, Melbourne, Australia

¹²Department of Pathology, and ¹⁴Department of Paediatrics, University of Melbourne, Melbourne, Australia

¹³Australian Genomics Health Alliance, Melbourne, Australia

¹⁵Department of Pediatrics, University of Oklahoma Health Sciences Center (OUHSC), Oklahoma, USA

¹⁶Department of Clinical Genomics, Mayo Clinic, Jacksonville, Florida, USA

¹⁷Genetic Medicine & Familial Cancer Centre, Royal Melbourne Hospital, Melbourne, Australia

Corresponding author:

Lisa G. Riley, PhD

Rare Diseases Functional Genomics

Kids Research

The Children's Hospital at Westmead

Locked Bag 4001, Westmead

NSW 2145 Australia

lisa.riley@health.nsw.gov.au

GRANTS

This research was supported by National Health and Medical Research Council of Australia (NHMRC) Project Grants APP1026891 and APP1068409. The Australian Genomics Health Alliance (*Australian Genomics*) project is funded by an NHMRC Targeted Call for Research grant (GNT1113531).

ABSTRACT

LARS2 variants are associated with Perrault syndrome, characterised by premature ovarian failure and hearing loss, and with an infantile lethal multi-system disorder: hydrops, lactic acidosis, sideroblastic anemia (HLASA) in one individual. Recently we reported *LARS2* deafness with (ovario) leukodystrophy. Here we describe five patients with a range of phenotypes, in whom we identified biallelic *LARS2* variants: three patients with a HLASA-like phenotype, an individual with Perrault syndrome whose affected siblings also had leukodystrophy, and an individual with a reversible mitochondrial myopathy, lactic acidosis and developmental delay.

Three HLASA cases from two unrelated families were identified. All were males with genital anomalies. Two survived multisystem disease in the neonatal period; both have developmental delay and hearing loss. A 55 year old male with deafness has not displayed neurological symptoms while his female siblings with Perrault syndrome developed leukodystrophy and died in their 30's. Analysis of muscle from a child with a reversible myopathy showed reduced *LARS2* and mitochondrial complex I levels, and an unusual form of degeneration. Analysis of recombinant *LARS2* variant proteins showed they had reduced amino-acylation efficiency, with HLASA-associated variants having the most severe effect. A broad phenotypic spectrum should be considered in association with *LARS2* variants.

Key words: Perrault syndrome; hydrops; lactic acidosis; sideroblastic anemia; leukodystrophy

INTRODUCTION

LARS2 encodes mitochondrial leucyl-tRNA synthetase which is responsible for the ATP-dependent conjugation of leucine to its cognate tRNA to support mitochondrial protein synthesis. Variants in mitochondrial aminoacyl-tRNA synthetases are associated with a broad range of mitochondrial disorders despite their common role in mitochondrial protein synthesis. The central nervous system (CNS) is affected in most mitochondrial aminoacyl-tRNA synthetase-related disease, with or without involvement of other organs, however a few of these disorders exclusively affect non-CNS tissues (Gonzalez-Serrano, Chihade, & Sissler, 2019). For some of the mitochondrial aminoacyl-tRNA synthetases two different phenotypes have been associated with biallelic variants e.g., *AARS2* infantile cardiomyopathy (MIM# 614096) (Götz et al., 2011), and leukoencephalopathy with premature ovarian failure (MIM# 615889) (Dallabona et al., 2014), or a wide range of disease severity has been reported e.g., *YARS2* MLASA2 (MIM# 613561) where some cases manifest isolated myopathy or sideroblastic anemia (Riley et al., 2018; Sommerville et al., 2017).

Most reports of disorders associated with *LARS2* variants report sensorineural hearing loss and premature ovarian failure (Perrault syndrome 4; MIM# 615300) (Demain et al., 2017; Lerat et al., 2016; Pierce et al., 2013). However, we have previously reported an individual with a lethal multi-system disorder comprising hydrops, lactic acidosis, and sideroblastic anemia (HLASA; MIM# 617021) with *LARS2* variants (Riley et al., 2016). More recently, individuals with Perrault syndrome and neurological symptoms caused by biallelic *LARS2* variants have been reported (Kosaki, Horikawa, Fujii, & Kosaki, 2018; van der Knaap et al., 2019). Here we report three additional HLASA cases from two unrelated families who begin to bridge the phenotypic spectrum of *LARS2*-associated disease, where one individual from each family has survived the neonatal period but has sensorineural hearing loss and

developmental delay. We also report a family where a male has biallelic *LARS2* variants and sensorineural hearing loss and two female siblings who had deafness and ovarioleukodystrophy. In a fourth family, an individual with biallelic *LARS2* variants had a reversible myopathy, lactic acidosis phenotype which has not previously been reported in association with *LARS2*, but has some features in common with *YARS2* MLASA2.

MATERIALS AND METHODS

Editorial policies and ethical considerations

This research and all procedures followed were in accordance with ethical standards and was approved by the Human Research Ethics Committee of the Children's Hospital at Westmead (ID number 10/CHW/114) and of the Royal Children's Hospital (ID numbers HREC/16/MH251 and HREC34228). Informed consent was obtained for all individuals sequenced in the study, and ethics approval for the use of control muscle samples.

Clinical information

Clinical histories for affected individuals are supplied in Supp. Materials and family pedigrees in Supp. Figure S1.

DNA sequencing and analysis

Patient 1- The proband had clinical genetic testing through GeneDx, a commercial genetic testing company. Patient and parental DNA underwent trio exome sequencing and data analysis by GeneDx. Variants were confirmed by Sanger sequencing.

Patient 2b – The proband (2b) was ascertained through the Australian Genomics Acute Care Study. Patient 2b and parental DNA underwent rapid trio exome sequencing using an

Ampliseq RDY exome kit, analysed on a Life Technologies Proton instrument using a P1 v3 chip at the New South Wales (NSW) Health Pathology Randwick Genomics Laboratory. Reads were aligned to the Human Genome Reference Sequence Hb19/GRCh37, and single nucleotide and short insertion/deletion variants identified using TorrentSuite v5.0.5 software. Data filtering was performed using a NATA-approved in-house pipeline (v2.0) based on Gemini v18 with annotation from the Variant Effect Predictor (VEP) and dbNSFP databases, and leverages family structure and known inheritance patterns.

Targeted sequencing of *LARS2* on stored DNA from the proband's deceased sibling (2a) was performed by the NSW Health Pathology Randwick Genomics Laboratory.

Patient 3 - Singleton exome sequencing of patient 3 was performed on a commercial basis at the Victorian Clinical Genetic Service laboratory on a Illumina HiSeq4000 using a Nextera Rapid Capture Exome Kit. Data was processed using Cpipe (Sadedin et al., 2015).

Patient 4 - This patient was included in a previously studied cohort of Complex I deficiency patients (Calvo et al., 2010). His DNA underwent singleton exome sequencing at the Broad Institute of MIT and Harvard using Illumina Capture Exome technology (v.1) supplemented with additional baits to capture mitochondrial DNA (mtDNA), in conjunction with Prof Vamsi Mootha and Dr Sarah Calvo. Data was mapped to NCBI hg19/GRCh37 human genome reference sequencing using BWA (Li & Durbin, 2009), and then targeted gene analysis was performed using GATK Best Practices recommendations (McKenna et al., 2010), HaplotypeCaller (DePristo et al., 2011; Van der Auwera et al., 2013), Variant Effect Predictor (McLaren et al., 2016), and Seqr (<https://seqr.broadinstitute.org/>). The exome data was analysed for high quality, autosomal recessive variants predicted as having

high/moderate impact on protein with a MAF<0.005. Analysis of mtDNA was performed as described previously (Lieber et al., 2013).

Patient genomic data are available from the corresponding author on reasonable request.

In silico predictions of the effect of variants on protein function were made using SIFT (v6.2.0; Kumar et al., 2009) and PolyPhen-2 (HumVar; Adzhubei et al., 2010). For all reported SIFT analyses, the final set of aligned sequences had a median conservation score of 3.0.

Cloning and leucyl-tRNA synthetase assays

Recombinant LARS2 proteins were produced to assess amino-acylation of the identified variants. *LARS2* (NM_015340.3) variants were introduced into the pET22b/LARS2 construct using site-directed mutagenesis (Yao, Wang, Wu, & Wang, 2003). N-terminal 6-His tagged wild-type (WT) and variant LARS2 were expressed and purified as previously described (Yao et al., 2003). Since leucylation in mitochondria follows rules similar to those for *E. coli* leucylation (Sohm et al., 2004), *E. coli* tRNA₅^{Leu}(UAA) was used as the amino-acylation substrate in these experiments. The sequence of *E. coli* tRNA₅^{Leu}(UAA) was cloned, transcribed and purified according to established procedures (Perret et al., 1990). *In vitro* leucylation of the tRNA^{Leu} transcript was performed as previously described (Sohm et al., 2003). Kinetic parameters for tRNA leucylation were determined from Lineweaver-Burk plots by varying *E. coli* tRNA^{Leu} transcript (from 0.2 to 2.4 μM) and WT or variant LARS2 (from 3 to 30 nM). Further, for WT and p.(Arg103His) LARS2, amino-acylation plateaus were obtained in the presence 0.65 μM of tRNA^{Leu} transcript and 20 nM of each LARS2

variant and two different ATP concentrations (0.5 and 2.5 mM). Data were expressed as the mean of at least two independent experiments \pm SEM.

Immunoblotting

Immunoblotting and densitometry were performed as previously described, with the following modifications: membranes were probed with a 1:250 dilution of anti-LARS2 (Abcam ab96221), 1:500 anti-OXPHOS (Abcam ab110411) or a 1:1000 dilution of anti-VDAC1 (Abcam ab14734), overnight at 4°C (Riley et al., 2013). Quantitation was performed using Image Studio Lite (Li-cor Biosciences). LARS2 and RC complex subunit intensities were normalized to VDAC1 intensities.

RESULTS

Clinical features of the *LARS2* phenotypic spectrum

Four probands with potentially pathogenic biallelic *LARS2* variants were identified by independent exome sequencing analyses. More detailed clinical histories are provided in the Supp. Materials and family pedigrees in Supp. Figure S1. Patients from two unrelated families (patient 1 and patients 2a & 2b) had similar clinical features and resembled those of a previously reported individual with HLASA (Table 1) (Riley et al., 2016). The severity of hydrops varied among cases. Lactic acidosis and anemia were present in all cases, with sideroblastic anemia confirmed in the two patients who had a bone marrow aspirate. Pulmonary hypertension was a common feature. These new HLASA cases were all male and had hypospadias. There were variable effects on liver, cardiac and renal systems. Patient 1 had neonatal cholestasis (Supp. Figure S2), while patients 2a and 2b had hepatosplenomegaly. Patient 1 and 2b were not as severely affected as the first reported

HLASA case and both survived the neonatal period. Lactic acidosis and anemia resolved in both children. They have sensorineural hearing loss and developmental delay.

Patient 3, a male, had sensorineural hearing loss and two sisters in their 30's with hearing loss, primary amenorrhoea, and onset of leukodystrophy in adulthood. His sisters died without a genetic diagnosis but their clinical features are similar to the recently reported *LARS2* deafness and ovarioleukodystrophy phenotype (van der Knaap et al., 2019).

Patient 4 with reversible myopathy, lactic acidosis, and developmental delay, had a unique *LARS2* phenotype with some features overlapping with mild *YARS2* MLASA2 presentations (Riley et al., 2018; Sommerville et al., 2017). He had an unusual form of muscle degeneration predominantly seen in neck muscle (Figure 1a).

Identification of *LARS2* variants

Exome sequencing identified biallelic variants in *LARS2* (NM_015340.3) in all patients. The *LARS2* variants, their allele frequency, inheritance, and *in silico* predictions of pathogenicity are shown in Table 2, and their conservation among species in Supp. Figure S3. Variants have been submitted to ClinVar <https://www.ncbi.nlm.nih.gov/ezproxy2.library.usyd.edu.au/clinvar/>; (submission ID: SUB6018179; SCV000994653-SCV000994660). The c.683G>A [p.(Arg228His)] variant identified in patient 1 has previously been reported *in trans* with another *LARS2* missense variant in an individual with deafness and ovarioleukodystrophy (van der Knaap et al., 2019). It is noteworthy that the c.1552G>A [p.(Asp518Asn)] variant is not rare and 6 homozygotes have been reported in the gnomAD database, all of whom are adults >45 years of age (Patient 4, Table 2). All results were confirmed by Sanger sequencing. Sanger sequencing of DNA from patient 2a who died

at day 1 confirmed that the same *LARS2* variants as 2b, the proband, were present. DNA was not available from the parents or affected siblings of patient 3, however Sanger sequencing of unaffected siblings confirmed the *LARS2* variants were in *trans*.

LARS2 encodes mitochondrial leucyl-tRNA synthetase, which is responsible for attaching leucine to its cognate tRNA for mitochondrial protein synthesis. Six of the identified missense variants lie within the catalytic domain of *LARS2*, p.(Asp438Gly) is localized in the non-functional editing domain which enhances the catalytic efficiency (Ye et al., 2015), while p.(Thr700Ile) lies in the anticodon binding domain (Figure 2).

Amino-acylation activity of *LARS2* variants

The effect of the *LARS2* variants on *LARS2* amino-acylation activity was investigated by measuring the attachment of radiolabelled leucine to an *E. coli* tRNA^{Leu} substrate by purified recombinant *LARS2* variants. No significant differences in the yield or solubility of the variant proteins were observed during their production, suggesting that none of the recombinant *LARS2* variants were misfolded during their production in *E. coli* (data not shown). The *LARS2* variants identified in these patients result in reduced tRNA^{Leu} amino-acylation efficiency (Table 2). The k_{cat}/K_m ratio is proportional to the catalytic efficiency of the enzyme and thus allows comparison of each variant with the wild-type *LARS2*. For the HLASA patients (patients 1, 2a, 2b), there was one *LARS2* variant with a severe effect on amino-acylation (>10-fold loss in catalytic efficiency) in combination with a variant with less effect on amino-acylation. The *LARS2* variants in patients 3 and 4 had milder effects on amino-acylation activity compared to the HLASA patients, consistent with their less severe phenotypes.

The p.(Arg228His) LARS2 variant identified in patient 1 caused a 48-fold loss in catalytic efficiency (Table 2), mainly due to a decreased k_{cat} value (Supp. Table S1) suggesting the variant hinders efficient transfer of the leucyl moiety from the active site to the 3' end of the tRNA (Figure 2). p.Arg228 is highly conserved, including in bacterial leucyl-tRNA synthetase (LeuS) alignments (Supp. Figure S3). LARS2 p.Arg228 is equivalent to p.Arg178 in *Thermus thermophilus* LeuS that binds the leucyl-adenylate analog and is important for the activity of the enzyme. In contrast, LARS2 p.Asp438 is not highly conserved, and the p.(Asp438Gly) variant found in patient 1 had little effect on amino-acylation efficiency (< 2-fold) compared to wild-type LARS2 (Table 2).

The p.(Ala130Thr) LARS2 variant found in patients 2a and 2b had a 16-fold decrease in amino-acylation efficiency (Table 2), again mainly due to a decreased k_{cat} value (Supp. Table S1). p.Ala130 lies in the catalytic domain and is highly conserved (Supp. Figure S3). In the crystal structure of the homologous *E. coli* LeuS-tRNA^{Leu} complex, the equivalent amino acid of p.Ala130 is located in close vicinity of A76, the last tRNA nucleotide where the leucyl moiety is attached after amino-acylation, and is probably involved in the catalytic process (Figure 2) (Palencia et al., 2012). LARS2 p.Thr700, located in the anticodon binding domain, is conserved in mammals but not in invertebrates and prokaryotes and the p.(Thr700Ile) variant found in patients 2a and 2b led to a 3-fold loss in catalytic efficiency (Table 2).

The p.(Pro536Leu) variant identified in patient 3, led to a 6-fold loss in catalytic efficiency. p.Pro536 is conserved in most species (Supp. Table S1). The p.(Gln147Pro) variant identified in patient 3 caused a 2-fold loss in amino-acylation efficiency compared to the WT LARS2 (Table 2). p.Gln147 is located in the catalytic domain but is not conserved.

For variants identified in patient 4, the recombinant LARS2 p.(Arg103His) had a <2-fold loss of catalytic efficiency and p.(Asp518Asn) had a 6-fold loss of efficiency (Table 2). p.Asp518 is located in the catalytic domain (Figure 2) and conserved in eukaryotes but may be replaced by Asn in some bacteria (e.g. *B. subtilis*, *S. aureus*, *M. mobile*). Moreover, there are six reported healthy homozygotes with the p.(Asp518Asn) variant in the gnomAD database. Given this, it was unexpected that p.(Arg103His) only showed a 1.6-fold loss in catalytic efficiency. Since p.Arg103 is highly conserved and located next to the HIGH (His-Ile-Gly-His) motif, responsible for ATP binding (Figure 2), additional experiments were performed to investigate the effect of the ATP concentration on the amino-acylation efficiency of the LARS2 p.(Arg103His) variant. The aminoacylation of tRNA^{Leu} by WT LARS2 was not affected in the presence of low ATP concentration *in vitro* (Figure 3). On the contrary, tRNA^{Leu} amino-acylation with the LARS2 p.(Arg103His) variant was reduced when ATP concentration was lowered to 0.5 mM (Figure 3). Reports of mitochondrial ATP concentrations are sparse and varied but have been reported at 2.5 mM in cultured human cells and as low as 0.5 mM in isolated rat hepatocytes (Soboll, Grundel, Schwabe, & Scholz, 1984; Yoshida, Kakizuka, & Imamura, 2016).

Muscle histopathology and immunoblotting

Further studies were undertaken for patient 4 who had a phenotype not previously reported in association with *LARS2* variants: myopathy, lactic acidosis and mitochondrial complex I enzyme deficiency in muscle, with improvement by adulthood. Muscle histopathology on biopsies taken at two years of age showed evidence of a mitochondrial myopathy (Figure 1a). A neck extensor muscle biopsy showed marked variation in muscle fiber size with many small degenerate fibers and some regenerating fibers. There was a mild increase in the

number of central nuclei, and mild peri-and endomysial fibrosis was seen. There was evidence of an unusual form of degeneration, with the Gomori trichome stain showing a flocculent grey granular appearance and accumulation of mitochondria, whilst the acid phosphatase stain also showed changes consistent with degeneration. Fiber typing showed a marked reduction of Type I fibers. Oil Red O staining revealed increased numbers of large droplets, many of which had irregular shapes. Quadriceps muscle showed mild variation of muscle fiber size, probably within normal limits (Figure 1a). There was no increase in central nuclei, but the Gomori trichome staining revealed subsarcolemmal accumulation of mitochondria, with other stains normal and indicative of a normal fiber type distribution.

The effect of the *LARS2* variants identified in patient 4 on endogenous levels of LARS2 protein and representative subunits of each of the respiratory chain (RC) complexes was also examined. Immunoblotting of LARS2 from patient 4 muscle showed levels of LARS2 were reduced to ~20% of age-matched control levels (Figure 1b). Complex I subunit NDUF8 levels in patient 4 muscle were reduced to ~12% of the control level, (Figure 1b), consistent with the reported isolated complex I enzyme deficiency in muscle. All other RC complex subunits were moderately reduced (II-SDHB 40%, III-UQCRC2 75%, IV-COX II 70%, V-ATP5A 65% of control). Immunoblotting of patient fibroblasts showed no change in LARS2 protein level and no effect on mitochondrial RC complex protein levels relative to control fibroblasts (results not shown).

DISCUSSION

Here we report the phenotypic spectrum of individuals from four families with biallelic *LARS2* sequence variants. The additional HLASA cases reported in this study confirm

HLASA as a *LARS2* phenotype and suggest that the three known *LARS2* phenotypes represent a spectrum of disease severity.

Patients 1, 2a and 2b in this study have clinical features consistent with HLASA, although hydrops was not as severe as the previously reported case. Abnormalities were detected *in utero* by ultrasound in all four HLASA cases, ranging from increased nuchal translucency, suspected fetal anemia, shortening of long bones and suspected micropenis to severe hydrops, and 3 of 4 cases were delivered prematurely due to fetal distress. All had respiratory distress and pulmonary hypertension at birth and required respiratory support. All four had severe lactic acidosis in the newborn period and were anemic. Many of the presenting clinical features of HLASA resolved in the two individuals who survived the neonatal period. Interestingly, micropenis/hypospadias was evident in three of these new cases, suspected on antenatal ultrasound. Hypospadias has only been previously reported in one *LARS2* Perrault syndrome case (Demain et al., 2017). Whereas ovarian dysgenesis is a defining feature of Perrault syndrome in females, most males are not reported to have genital anomalies or subfertility. Endocrine investigations in patient 2b at age 4 months were normal for age with no evidence of gonadal failure. These additional HLASA patients confirm hypospadias as a *LARS2* phenotype and the surviving patients who have sensorineural hearing loss, developmental delay, and male external genital anomalies suggest HLASA may represent the severe end of the Perrault syndrome spectrum.

Recently cases of *LARS2*-associated Perrault syndrome with neurological symptoms have been reported (Kosaki et al., 2018; van der Knaap et al., 2019). In five of six of these patients developmental delay was present, as in the surviving HLASA cases, and one patient was reported to be small for gestational age. Leukodystrophy was confirmed in three patients.

These patients developed neurological features anywhere from early childhood to 45 years of age. In this study, the female siblings of patient 3 had Perrault syndrome and leukodystrophy, with neurological features presenting at 28 and 34 years of age while patient 3 has no neurological symptoms at age 55 years. While the female siblings did not have genetic testing, it is probable that they have the same genotype as their brother but with a more severe phenotype, suggesting *LARS2*-associated disease may be affected by genetic and/or environmental modifiers, and that long-term monitoring for new neurological features is required in all patients. The phenotypic features of families 1, 2 and 3 are all on the *LARS2* phenotypic spectrum and the severity of disease correlates somewhat with the degree of loss of amino-acylation activity caused by the variants involved.

Phenotypic variability is common in Perrault syndrome, which is caused by variants not only in *LARS2* but also *HARS2* (MIM# 614926), *TWINK* (MIM# 616138), *CLPP* (MIM# 614129), *ERAL1* (MIM# 617565), and *HSD17B4* (MIM# 233400) (Newman, Friedman, & Conway, 1993). Most of these genes are involved in mitochondrial proteostasis, suggesting common pathways may be impacted. A wide phenotypic spectrum has also been observed in *HSD17B4*-associated disease that ranges from Perrault syndrome to D-bifunctional protein deficiency (MIM# 261515) which is a severe, usually infantile lethal disease (Pierce et al., 2010). The severity of disease is related to the level of dysfunction caused by *HSD17B4* variants and the functional domain in which the variants are located. Similarly, in this study *LARS2* variants associated with HLASA had a more severe effect on amino-acylation than those in the less severe phenotypes. Neurological symptoms have been reported in Perrault syndrome associated with variants in *TWINK*, *CLPP*, and *HSD17B4* as well as *LARS2* (Demain et al., 2017; Kosaki et al., 2018; Lerat et al., 2016; van der Knaap et al., 2019). A few cases of male infertility (azoospermia) have been reported in males with *CLPP* and

HSD17B4 variants, and both male and female *CLPP* knockout mice are sterile (Demain et al., 2017; Lerat et al., 2016). A male with *LARS2* Perrault syndrome had hypospadias while his sister had oligomenorrhoea with a small uterus and ovaries (Demain et al., 2017). A strain of *C. elegans* with a homozygous protein-truncating *LARS2* variant was sterile, and had smaller gonads than wild-type controls (Pierce et al., 2013). This study indicates that male external genital anomalies can occur in *LARS2*-associated disease, and male gonadal dysgenesis could also occur but may be underreported in *LARS2* Perrault syndrome.

There is also phenotypic overlap between *LARS2*-associated disorders and those caused by other mitochondrial aminoacyl-tRNA synthetases. *HARS2* variants are also associated with Perrault syndrome (Pierce et al., 2011). There is some phenotypic overlap between some *LARS2* cases and patients with variants in *MARS2* and *AARS2*, encoding mitochondrial methionyl- and alanyl-tRNA synthetases respectively. Variants in *MARS2* cause autosomal recessive spastic ataxia with leukoencephalopathy (ARSAL; MIM# 611390) and developmental delay and sensorineural hearing loss (MIM# 616430) (Bayat et al., 2012; Webb et al., 2015). Variants in *AARS2* have been associated with leukodystrophy and premature ovarian failure (Dallabona et al., 2014). *YARS2* variants cause myopathy, lactic acidosis and sideroblastic anemia (MLASA2) and severe cases bear some similarity to HLASA while mild cases bear some similarity to the phenotype of patient 4 (Riley et al., 2018; Riley et al., 2013; Sommerville et al., 2017). In some MLASA2 cases sideroblastic anemia resolved, as seen in patient 1 and 2b (Riley et al., 2018).

The phenotype of patient 4 included early developmental delay and lactic acidosis in common with patients 1 and 2b, but he also had reversible infantile-onset myopathy which has not previously been reported in association with *LARS2* variants. Interestingly, the

myopathy was most severe in the neck muscles, which are derived from a different lineage and regulated by distinct genetic programs compared to other muscle types (e.g., quadriceps) (Heude et al., 2018). The unusual features of this patient may be related to the combination of *LARS2* missense variants, one of which has reduced amino-acylation efficiency at low ATP concentrations, or could be a result of genetic and/or environmental factors. However, it is difficult to assess the limit at which a variant causes a phenotype *in vivo* based on the loss of efficiency as it does not always correlate with disease severity (Gonzalez-Serrano et al., 2019). It should therefore be kept in mind that in addition to a slight effect on amino-acylation, these variants could also alter the stability of the protein *in vivo* or its transport into the mitochondria and worsen the defect. Indeed, the immunoblot of patient 4 muscle showed a reduction in *LARS2* protein level while there was no observable difference in protein expression or stability of the recombinant variants. Similarly, we cannot exclude that some *LARS2* variants may differentially affect the amino-acylation of the two mt-tRNA^{Leu} isoacceptors encoded by the mitochondrial genome which may explain some discrepancies in the observed phenotypes. The patient's symptoms had largely resolved by adolescence, raising the possibility that the individuals in the gnomAD database homozygous for the p.(Asp518Asn) variant may have a very mild phenotype which has gone clinically unrecognised. Some other reversible infantile mitochondrial diseases associated with mitochondrial translation defects have been described (Boczonadi, Bansagi, & Horvath, 2015).

In conclusion, we expand the clinical spectrum of *LARS2*-associated mitochondrial disease to include infantile lethal HLASA, infantile HLASA resolving to developmental delay and hearing loss, hypospadias in males, hearing loss with premature ovarian failure (Perrault syndrome), hearing loss with ovarioleukodystrophy, and reversible infantile-onset myopathy.

We recommend these possible phenotypes be considered in association with *LARS2* variants and monitoring of patients for development of these clinical features.

DATA AVAILABILITY STATEMENT

Patient genomic data are available from the corresponding author on reasonable request.

Variants reported in this study have been deposited in ClinVar <https://www.ncbi.nlm.nih.gov/ezproxy2.library.usyd.edu.au/clinvar/> ; submission ID: SUB6018179.

ACKNOWLEDGEMENTS

We are indebted to Enduo Wang (Shanghai) for the generous gift of a *LARS2* clone. We thank Lucy Kevin, CHW Genetic Counsellor for assistance with coordination of genetic investigations for Patients 2a and 2b, and George Elakis, Sarah Lang and Anna Richards, NSW Health Pathology Randwick, for technical assistance provided in enabling the rapid diagnosis of Patient 2b. This research was supported by National Health and Medical Research Council of Australia (NHMRC) Project Grants APP1026891 and APP1068409. The Australian Genomics Health Alliance (*Australian Genomics*) project is funded by an NHMRC Targeted Call for Research grant (GNT1113531). Additional support to the Acute Care flagship was provided from the estate of the Late JH Thomas to Kids Research, Sydney Children's Hospitals Network (Randwick and Westmead). Research conducted at Kids Research was supported by the Luminesce Alliance – Innovation for Children's Health, a not for profit cooperative joint venture between the Sydney Children's Hospitals Network, the Children's Medical Research Institute, and the Children's Cancer Institute. It has been established with the support of the NSW Government to coordinate and integrate paediatric research. Luminesce Alliance is also affiliated with the University of Sydney and the University of New South Wales Sydney. This work was supported by the CNRS and the

Université de Strasbourg. The research conducted at the Murdoch Children's Research Institute was supported by the Victorian Government's Operational Infrastructure Support Program. We are grateful to the Crane and Perkins families for their generous financial support. The authors declare that they have no conflicts of interest.

CONFLICT OF INTEREST

The authors declare that they have no conflicts of interest

AUTHOR CONTRIBUTIONS

LGR performed patient 4 Sanger sequencing, *in silico* predictions, immunoblotting, cloning and wrote the manuscript; JR-T and MF designed and performed *in vitro* aminoacylation assays; KW and SP provided clinical history, diagnosis and management of patient 1; MWilson, ML, TIA, provided clinical history, diagnosis and management of patient 2a/b, CYN, TR, EK, SL, ZS provided genomic analysis of patient 2a/b; MWalsh and EH coordinated research consents and sample collection, and provided clinical history, diagnosis and management of patient 3; ST and AGC extracted patient 4 DNA for exome sequencing, curated the exome data and performed some confirmatory experiments; SA muscle histopathology for patient 4; DRT provided mitochondrial RC enzyme activities for patient 4; JC provided clinical history, diagnosis and management of patient 4, obtained consent and samples for the study and contributed to the overall conception and progression of the study. All authors contributed to editing the manuscript.

REFERENCES

- Adzhubei, I.A., Schmidt, S., Peshkin, L., Ramensky, V.E., Gerasimova, A. Bork, P., . . . Sunyaev, S.R. (2010). A method and server for predicting damaging missense mutations. *Nature Methods*, 7, 248-249.
- Bayat, V., Thiffault, I., Jaiswal, M., Tetreault, M., Donti, T., Sasraman, F., . . . Bellen, H. (2012). Mutations in the mitochondrial methionyl-tRNA synthetase cause a neurodegenerative phenotype in flies and a recessive ataxia (ARSAL) in humans. *PLoS Biology*, 10, 1-19.
- Boczonadi, V., Bansagi, B., & Horvath, R. (2015). Reversible infantile mitochondrial diseases. *Journal of Inherited Metabolic Disease*, 38, 427-435.
- Calvo, S. E., Tucker, E. J., Compton, A. G., Kirby, D. M., Crawford, G., Burt, N. P., . . . Mootha, V. K. (2010). High-throughput, pooled sequencing identifies mutations in NUBPL and FOXRED1 in human complex I deficiency. *Nature Genetics*, 42, 851-858.
- Dallabona, C., Diodato, D., Kevelam, S., Haack, T., Wong, L. J., Salomons, G., . . . van der Knaap, M. (2014). Novel (ovario) leukodystrophy related to *AARS2* mutations. *Neurology*, 82, 2063-2071.
- Demain, L. A., Urquhart, J. E., O'Sullivan, J., Williams, S. G., Bhaskar, S. S., Jenkinson, E. M., . . . Newman, W. G. (2017). Expanding the genotypic spectrum of Perrault syndrome. *Clinical Genetics*, 91, 302-312.
- DePristo, M. A., Banks, E., Poplin, R., Garimella, K. V., Maguire, J. R., Hartl, C., . . . Daly, M. J. (2011). A framework for variation discovery and genotyping using next-generation DNA sequencing data. *Nature Genetics*, 43, 491-498.
- Gonzalez-Serrano, L. E., Chihade, J. W., & Sissler, M. (2019). When a common biological role does not imply common disease outcomes: Disparate pathology linked to human

- mitochondrial aminoacyl-tRNA synthetases. *Journal of Biological Chemistry*, 294, 5309-5320.
- Götz, A., Tyynismaa, H., Euro, L., Ellonen, P., Hyötyläinen, T., Ojala, T., . . . Suomalainen, A. (2011) Exome sequencing identifies mitochondrial alanyl-tRNA synthetase mutations in infantile mitochondrial cardiomyopathy. *American Journal of Human Genetics*, 88, 635-642.
- Heude, E., Tesarova, M., Sefton, E. M., Jullian, E., Adachi, N., Grimaldi, A., . . . Tajbakhsh, S. (2018). Unique morphogenetic signatures define mammalian neck muscles and associated connective tissues. *Elife*, 7. doi:10.7554/eLife.40179
- Kosaki, R., Horikawa, R., Fujii, E., & Kosaki, K. (2018). Biallelic mutations in LARS2 can cause Perrault syndrome type 2 with neurologic symptoms. *American Journal of Medical Genetics A*, 176, 404-408.
- Kumar, P., Henikoff, S., & Ng, P.C. (2009). Predicting the effects of coding non-synonymous variants on protein function using the SIFT algorithm. *Nature Protocols*, 4, 1073-1082.
- Lerat, J., Jonard, L., Loundon, N., Christin-Maitre, S., Lacombe, D., Goizet, C., . . . Marlin, S. (2016). An Application of NGS for Molecular Investigations in Perrault Syndrome: Study of 14 Families and Review of the Literature. *Human Mutation*, 37, 1354-1362.
- Li, H., & Durbin, R. (2009). Fast and accurate short read alignment with Burrows-Wheeler transform. *Bioinformatics*, 25, 1754-1760.
- Lieber, D. S., Calvo, S. E., Shanahan, K., Slate, N. G., Liu, S., Hershman, S. G., . . . Mootha, V. K. (2013). Targeted exome sequencing of suspected mitochondrial disorders. *Neurology*, 80, 1762-1770.

- McKenna, A., Hanna, M., Banks, E., Sivachenko, A., Cibulskis, K., Kernytsky, A., . . .
- DePristo, M. A. (2010). The Genome Analysis Toolkit: a MapReduce framework for analyzing next-generation DNA sequencing data. *Genome Research*, *20*, 1297-1303.
- McLaren, W., Gil, L., Hunt, S. E., Riat, H. S., Ritchie, G. R., Thormann, A., . . .
- Cunningham, F. (2016). The Ensembl Variant Effect Predictor. *Genome Biology*, *17*, 122.
- Newman, W. G., Friedman, T. B., & Conway, G. S. (2014). Perrault Syndrome. In R. A. Pagon, M. P. Adam, H. H. Ardinger, S. E. Wallace, A. Amemiya, L. J. H. Bean, T. D. Bird, N. Ledbetter, H. C. Mefford, R. J. H. Smith, & K. Stephens (Eds.), *GeneReviews(R)*. Seattle (WA): University of Washington, Seattle; 1993-2020.
- Palencia, A., Crépin, T., Vu, M. T., Lincecum, T. L., Jr., Martinis, S. A., & Cusack, S. (2012). Structural dynamics of the aminoacylation and proofreading functional cycle of bacterial leucyl-tRNA synthetase. *Nature Structural and Molecular Biology*, *19*, 677-684.
- Perret, V., Garcia, A., Grosjean, H., Ebel, J. P., Florentz, C., & Giegé, R. (1990). Relaxation of a transfer RNA specificity by removal of modified nucleotides. *Nature*, *344*, 787-789.
- Pierce, S. B., Chisholm, K. M., Lynch, E. D., Lee, M. K., Walsh, T., Opitz, J. M., . . . King, M. C. (2011). Mutations in mitochondrial histidyl tRNA synthetase HARS2 cause ovarian dysgenesis and sensorineural hearing loss of Perrault syndrome. *Proceedings of the National Academy of Sciences U S A*, *108*, 6543-6548.
- Pierce, S. B., Gersak, K., Michaelson-Cohen, R., Walsh, T., Lee, M. K., Malach, D., . . . Levy-Lahad, E. (2013). Mutations in LARS2, encoding mitochondrial leucyl-tRNA synthetase, lead to premature ovarian failure and hearing loss in Perrault syndrome. *American Journal of Human Genetics*, *92*, 614-620.

- Pierce, S. B., Walsh, T., Chisholm, K. M., Lee, M. K., Thornton, A. M., Fiumara, A., . . . King, M. C. (2010). Mutations in the DBP-deficiency protein HSD17B4 cause ovarian dysgenesis, hearing loss, and ataxia of Perrault Syndrome. *American Journal of Human Genetics*, *87*, 282-288.
- Riley, L. G., Heeney, M. M., Rudinger-Thirion, J., Frugier, M., Campagna, D. R., Zhou, R., . . . Fleming, M. D. (2018). The phenotypic spectrum of germline YARS2 variants: from isolated sideroblastic anemia to mitochondrial myopathy, lactic acidosis and sideroblastic anemia 2. *Haematologica*, *103*, 2008-2015.
- Riley, L. G., Menezes, M. J., Rudinger-Thirion, J., Duff, R., de Lonlay, P., Rotig, A., . . . Christodoulou, J. (2013). Phenotypic variability and identification of novel YARS2 mutations in YARS2 mitochondrial myopathy, lactic acidosis and sideroblastic anaemia. *Orphanet Journal of Rare Diseases*, *8*, 193.
- Riley, L. G., Rudinger-Thirion, J., Schmitz-Abe, K., Thorburn, D. R., Davis, R. L., Teo, J., . . . Christodoulou, J. (2016). LARS2 Variants Associated with Hydrops, Lactic Acidosis, Sideroblastic Anemia, and Multisystem Failure. *Journal of Inherited Metabolic Disease Reports*, *28*, 49-57.
- Sadedin, S. P., Dashnow, H., James, P. A., Bahlo, M., Bauer, D. C., Lonie, A., . . . Thorne, N. P. (2015). Cpipe: a shared variant detection pipeline designed for diagnostic settings. *Genome Medicine*, *7*, 68. doi:10.1186/s13073-015-0191-x
- Soboll, S., Grundel, S., Schwabe, U., & Scholz, R. (1984). Influence of fatty acids on energy metabolism. 2. Kinetics of changes in metabolic rates and changes in subcellular adenine nucleotide contents and pH gradients following addition of octanoate and oleate in perfused rat liver. *European Journal of Biochemistry*, *141*, 231-236.

- Sohm, B., Sissler, M., Park, H. King, M.P. & Florentz, C. (2004). Recognition of human mitochondrial tRNA^{Leu(UUR)} by its cognate leucyl-tRNA synthetase. *Journal of Molecular Biology*, 339,17-29.
- Sohm, B., Frugier, M., Brulé, H., Olszak, K., Przykorska, A., & Florentz, C. (2003). Towards understanding human mitochondrial leucine aminoacylation identity. *Journal of Molecular Biology*, 328, 995-1010.
- Sommerville, E. W., Ng, Y. S., Alston, C. L., Dallabona, C., Gilberti, M., He, L., . . . Gorman, G. S. (2017). Clinical Features, Molecular Heterogeneity, and Prognostic Implications in YARS2-Related Mitochondrial Myopathy. *JAMA Neurology*, 74, 686-694.
- Van der Auwera, G. A., Carneiro, M. O., Hartl, C., Poplin, R., Del Angel, G., Levy-Moonshine, A., . . . DePristo, M. A. (2013). From FastQ data to high confidence variant calls: the Genome Analysis Toolkit best practices pipeline. *Current Protocols in Bioinformatics*, 43, 11.10.11-33.
- van der Knaap, M. S., Bugiani, M., Mendes, M. I., Riley, L. G., Smith, D. E. C., Rudinger-Thirion, J., . . . Mochel, F. (2019). Biallelic variants in LARS2 and KARS cause deafness and (ovario)leukodystrophy. *Neurology*, 92(11), e1225-e1237.
doi:10.1212/wnl.0000000000007098
- Webb, B., Wheeler, P., Hagen, J., Cohen, N., Linderman, M., Diaz, G., . . . Schadt, E. (2015). Novel, compound heterozygous, single nucleotide variants in MARS2 associated with developmental delay, poor growth, and sensorineural hearing loss. *Human Mutation*, 36, 587-592.
- Yao, Y., Wang, L., Wu, X., & Wang, E. (2003). Human mitochondrial leucyl-tRNA synthetase with high activity produced from *Escherichia coli*. *Protein Expression and Purification*, 30, 112-116.

Ye, Q., Wang, M., Fang, Z., Ruan, Z., Ji, Q, Zhou, Z & Wang. E. (2015). Degenerate connective polypeptide 1 (CP1) domain from human mitochondrial leucyl-tRNA synthetase. *Journal of Biological Chemistry*, 290, 24391-24402.

Yoshida, T., Kakizuka, A., & Imamura, H. (2016). BTeam, a Novel BRET-based Biosensor for the Accurate Quantification of ATP Concentration within Living Cells. *Science Reports*, 6, 39618. doi:10.1038/srep39618

FIGURE LEGENDS

Figure 1. Analyses of Patient 4 muscle biopsies. **(a)** Histological findings. Haemotoxylin and eosin staining of neck extensor (i) and quadriceps (ii) Gomori trichrome staining of neck extensor (iii) and quadriceps (iv) NADH staining of neck extensor (v) and quadriceps (vi). Acid phosphatase staining of neck extensor (vii). Images taken at 20× magnification except (v) and (vii) at 40×. **(b)** Immunoblot for LARS2 and subunits of the RC complexes (I – NDUFB8, II-SDHB, III-UQCRC2, IV-COX II, V-ATP5A) in patient 4 (P4) and age-matched control (C1) muscle replicates. Note that these RC complex subunits are labile if their complex is not assembled. VDAC1 was used as a loading control.

Figure 2. Localisation of LARS2 variants on the crystal structure of the *E. coli* LeuS/tRNA^{Leu} complex (PDB: 4AQ7). **(a)** LARS2 is a class I ARS homologous to *E. coli* LeuS which displays a catalytic domain (cyan), an editing domain (orange) and a C-terminal tRNA binding domain (grey). The catalytic domain binds ATP (red) and leucine (green) to form leucyl-adenylate. The leucyl moiety is then transferred to the 3' end of tRNA^{Leu} (magenta). In *E. coli*, the editing domain is involved in the hydrolysis of mischarged tRNA^{Leu} (mainly with isoleucine) to ensure translation fidelity. This domain does not function as an editing domain in LARS2 but is crucial in enhancing the catalytic efficiency. Similarly, the zinc (dark blue) binding domain is not functional in LARS2. *E. coli* LeuS nucleotides equivalent to LARS2 variants are underlined by yellow spheres. They correspond to LARS2 p.(Arg103) (*E. coli* Arg54), LARS2 p.(Ala130) (*E. coli* Ala81), LARS2 p.(Gln147) (*E. coli* Ala98), LARS2 p.(Arg228) (*E. coli* Arg178), LARS2 p.(Asp438) (*E. coli* Gly409), LARS2 p.(Asp518) (*E. coli* Asp488), LARS2 p.(Pro536) (*E. coli* Pro506) and LARS2 p.(Thr700) (*E.*

coli Tyr678). (b) Close up of the catalytic domain of *E. coli* LeuS highlighting variants that affected amino-acylation with a >3-fold loss in catalytic efficiency.

Figure 3. Effect of ATP concentration on WT and p.(Arg103His) LARS2 enzymatic activities. Leucylation reactions were carried out using 0.5 (●) or 2.5 mM (○) ATP in the presence of 0.65 μ M tRNA^{Leu} transcript and 20 nM of wild-type (blue) and p.(Arg103His) (red) enzymes. Values are mean (SEM), n = 3.

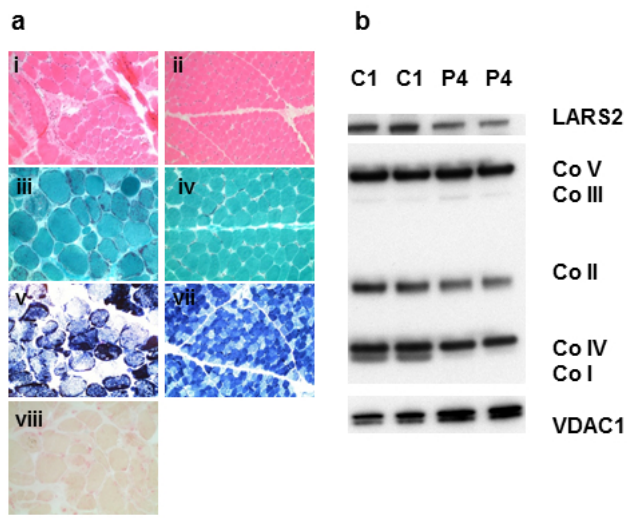


Figure 1

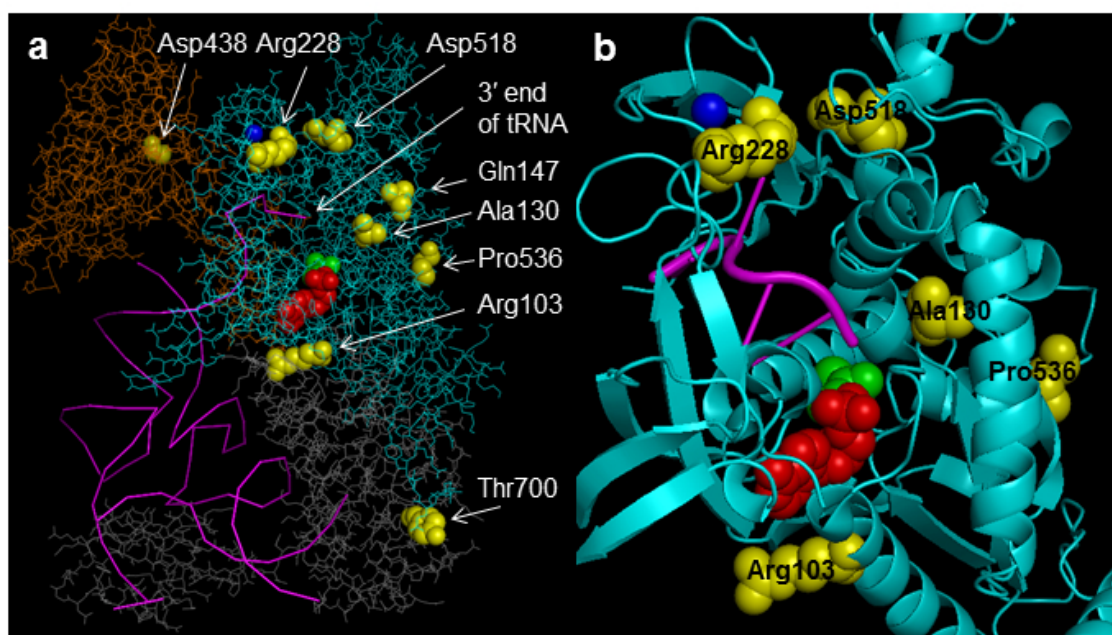


Figure 2

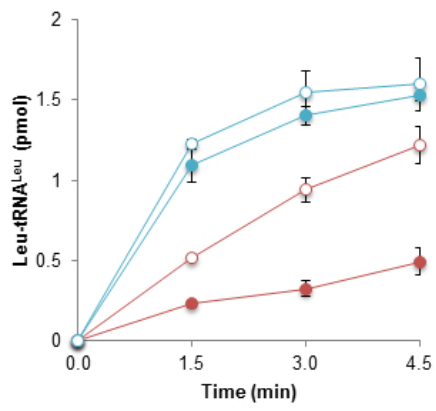


Figure 3

SUPPLEMENTARY MATERIALS

Clinical Histories

Patient 1

The male proband was the first child of a Japanese mother and a Caucasian father. Early antenatal scans raised concerns of intrauterine growth retardation (~ 3 weeks delay in growth) and genitalia anomalies. Amniocentesis performed in Japan showed a 46 XY karyotype although on ultrasound the genitalia looked female, so there was a suspicion the baby had a micropenis and severe hypospadias. After 21 weeks gestation the parents moved to the United States where an antenatal scan showed a massive pericardial effusion with severe pulmonary hypoplasia. No ascites or fluid elsewhere was noted. Repeat amniocentesis done in the USA was negative for Toxoplasmosis, CMV, and Parvovirus, and repeat karyotype showed 46, XY. On close follow up the pericardial effusion resolved over the following few weeks and the baby was born at 37 weeks of gestation with a birth weight of 1825 g.

At birth the baby had respiratory distress requiring surfactant, was placed on a high frequency oscillation ventilator, and given inhaled nitric oxide for concerns of hyaline membrane disease. He was weaned off respiratory support and did not develop chronic lung disease. He required vasopressor support for low blood pressure soon after birth. An echocardiogram confirmed pulmonary hypertension. By the time of neonatal ICU discharge all cardiac issues had resolved. He had no seizures with normal brain MRI. Also, at birth clinical examination and investigations showed ascites and anemia. Ascites was managed conservatively and resolved within 2 weeks. Anemia was non-hemolytic treated with transfusions and iron supplementation during the neonatal period.

Endocrinological testing during the neonatal period showed FSH was less than 1.2 IU/L, LH was less than 0.1 IU/L, Free T4 was 1.14 ng/dL (0.7-1.5ng/dL), TSH was 3.289 micro IU/mL (0.350-4.940 micro IU/mL), Testosterone 67 ng/dL, IGF-1 38 ng/mL, not discriminating for Growth Hormone deficiency at this age. The baby was on total parenteral nutrition for 2 weeks, tolerated breast feeds and Neosure 24 cal/30 ml formula. During his NICU stay direct hyperbilirubinemia was noted with max direct bilirubin of 3.7 mg/dL (0.1-0.5 mg/dL). A hepatobiliary (HIDA) scan did not show any excretion at 24 h.

At 6 weeks of age he was admitted for further investigation of his neonatal cholestasis. Testing showed a normal alpha-1 antitrypsin MM phenotype, and a neonatal cholestasis gene panel did not identify any pathogenic variants associated with PFIC 1, 2 or 3. An intra-operative cholangiogram showed excretion ruling out biliary atresia. A liver biopsy was performed and demonstrated paucity of bile ducts (Supp. Figure S2). His cholestasis slowly resolved.

At 9 months of age he was readmitted for severe anemia requiring blood transfusion, lactic acidosis, diarrhea and poor weight gain. His bone marrow biopsy showed ring sideroblasts. Lactic acidosis corrected with intravenous fluids. Due to poor weight gain he was started on gastrostomy feeds. His stool studies showed low fecal elastase suggestive of exocrine pancreatic insufficiency and hence he was started on Pancreatic Enzyme Replacement Therapy (PERT).

In view of multi-system involvement exome sequencing testing was undertaken. In addition to biallelic *LARS2* variants, a heterozygous *IGF2*, c.472delC, p.(Leu158*) variant was identified and a *MT-ATP6*, m.9029A>G, p.(His168Arg) variant at 15% heteroplasmy in both the patient and his mother.

At 2 years he has failure to thrive and remains on gastrostomy feeds consisting of Peptamen Junior bolus feeds during the day and continuous feeds at night. Due to feeding difficulties and concerns of aspiration he is receiving speech therapy twice a week. He remains on PERT for exocrine pancreatic insufficiency but has no other endocrine issues. An MRI of the abdomen showed no changes in the pancreas. He has elevated transaminases (AST 82 units/L (12-30 units/L), ALT 72 units/L (12-30 units/L)). Cholestasis has resolved and liver synthetic function is normal. He has moderate global developmental delay: walks without support 10 steps, can sit unaided, can stack blocks, and has limited vocabulary (only says mama and dada). He has sensorineural hearing loss and has received cochlear implants. He is awaiting hypospadias repair. His anemia and lactic acidosis have resolved. Neurologically he has had no seizures. He has no respiratory, cardiac or renal health concerns.

Patients 2a & 2b

These two male babies were born to unrelated, healthy parents of Middle Eastern background.

Their first baby (Patient 2a), a son, died at one day of age after delivery by emergency Caesarean section at 33 weeks for fetal distress. There had been an increased nuchal translucency (NT) measurement (3.3 mm) at 13 weeks, but a fetal morphology scan at 19 weeks was reportedly normal, apart from mildly short limbs. Amniocentesis showed a normal chromosome microarray. The mother developed flu like symptoms from 30 weeks gestation with multiple presentations to medical services, and was delivered by emergency caesarean section at 33 weeks for a non-reassuring fetal heart rate on cardiotocograph. The severity of illness at birth was unexpected. The child had severe anemia (Hb 53 g/L; normal range 142 to 240 g/L), lactic acidosis (highest lactate 24 mmol/L; normal range <2.0 mmol/L), severe hypoglycaemia (1.5 mmol/L; normal range 3.5 to 5.4 mmol/L), high insulin (22.3 mIU/L; normal <9 mIU/L) and low cortisol (36 nmol/L; critical low < 80 nmol/L). Clinical examination documented facial purpura, hepatosplenomegaly and micropenis. He had multiple blood transfusions but had continuing hypoxic respiratory failure unresponsive to maximal intensive care, and succumbed at one day of age. Blood group was A negative (maternal blood group A positive) and Coombs test negative, as was Kleihauer, TORCH and parvovirus testing. A 60K chromosome microarray (CMA) was normal. Post mortem was declined but the parents consented to DNA storage.

In the next pregnancy a cell-free DNA non-invasive pregnancy screening predicted a normal XY male (Patient 2b), but the NT was elevated (4.7 mm) and the couple was referred to the genetics service at 14 weeks gestation. There was significant concern about the likelihood of recurrence of an as yet undiagnosed genetic condition, but the couple did not want invasive testing without certainty about interpretability. Stored DNA from the first pregnancy was eventually sourced from the CMA test laboratory. A 51 gene congenital anemia panel was arranged through a commercial laboratory on Patient 2a and parental DNA. The results available after 22 weeks were uninformative (this included multiple genes associated with

Diamond-Blackfan anemia, congenital dyserythropoietic anemia, and sideroblastic anemia, but not the *YARS2* or *LARS2* genes).

Evidence of fetal anemia and fetal hydrops were detected at 17 weeks of gestation with an elevated middle cerebral artery peak systolic flow velocity (MCA PSV) of 47 cm/sec, polyhydramnios and pericardial effusion. A fetal echocardiogram showed an otherwise structurally normal heart. A femur length <5th centile and micropenis were noted at 19 weeks on ultrasound. Progress scans showed a stable MCA PSV suggesting mild to moderate fetal anemia, resolution of pericardial effusion and polyhydramnios. Progress growth scans revealed shortened proximal long bones at <3rd centile, normal fetal head measurements, hepatomegaly and a simple liver cyst. The MCA PSV was noted to increase to 60 cm/sec at 33 weeks with mild fetal ascites suggesting a worsening of fetal anemia. An emergency LSCS was performed for non-reassuring fetal heart rate.

The baby boy was delivered with Apgars of 4¹ and 6⁵, weight 1764 g (34th centile), length 41 cm (24th centile) and head circumference 31.5cm (85th centile). He had anemia (Hb 71 g/L; normal 142 to 240 g/L), initial high reticulocyte count, lactic acidosis with gross lactic aciduria (initial cord arterial lactate was 8.9 mmol/L, highest blood lactate 10.9 mmol/L an hour after birth; normal lactate <2.0 mmol/L), pulmonary hypertension, hypoglycemia (1.9 mmol/L; normal 3.5 to 5.4 mmol/L) with low cortisol (<30 nmol/L; critical low <80 nmol/L) and hyperinsulinism (10 mIU/L; normal <9 mIU/L). He had hepatosplenomegaly, penoscrotal hypospadias and undescended testes but no other anomalies. Peripheral blood film from a pre-transfusion sample showed a regenerative anemia with marked erythroblastosis, mild dyserythropoiesis and mild nuclear-cytoplasmic asynchrony. Mature red cells showed anisopoikilocytosis with tiny microcytes, tear drops, spherocytes and fragments. The total white cell and platelet counts were normal on initial film, although the initial neutrophil count was low. No ring sideroblasts were seen. Blood group was O positive, Coombs test negative, red blood cell enzyme levels normal and maximum serum bilirubin 8.77 mg/dL during the newborn period with otherwise normal liver function tests.

He had respiratory distress syndrome with pulmonary hypertension, requiring ventilation from birth, surfactant replacement, two blood transfusions in the first day, inhaled nitric oxide, vasopressor support for low blood pressure, and hydrocortisone for low cortisol levels. The lactic acidosis resolved by 12 hours of age, the pulmonary hypertension by 25 hours, and ventilation support needs decreased rapidly, with extubation to CPAP after 2 days, and CPAP ceased at day 6. He received phototherapy commencing on day 2. He required a further transfusion at day 14 but no further transfusion has been required since. He had a small PDA which resolved spontaneously but no other cardiac anomalies. His Hb gradually normalised and blood film morphology was normal by corrected age 6 months except for a relative macrocytosis. A bone marrow examination is planned when he has surgery for other reasons.

His newborn hearing screen was abnormal and profound sensorineural deafness was confirmed at age 2 months. ACTH stimulation responses were suboptimal on day 5 but normal by day 16 and hydrocortisone ceased. Steroid hormone profiles including testosterone were normal at 3 months. An MRI brain at corrected age 6 months showed mild generalised cerebral atrophy, and thin corpus callosum but normal myelination and normal inner and middle ear anatomy. At 7.5 months (corrected age 6 months) his length was 67 cm (37th centile), weight 7.3 kg (4th centile) and head circumference 44.5 cm (63rd centile). He was feeding well on bottle and purees, visually alert, smiling and vocalising, with symmetrical

and vigorous arm and leg movements but central hypotonia and not yet sitting unsupported. He underwent cochlear implants at 10 months of age.

Patient 3

The proband presented to a genetic service at 55 years of age. He had congenital-onset profound sensorineural hearing loss but no other health issues nor any learning difficulties. The proband was the only son of six children to his unrelated parents. Two of his sisters were born with sensorineural hearing loss and developed primary amenorrhea that was thought to be due to primary ovarian failure. They were otherwise healthy with no learning difficulties. At the age of 28 one of the sisters became unsteady on her feet and over 22 months she developed progressive cognitive impairment, weakness, spasticity and ataxia and died at the age of 30. Her MRI brain showed extensive white matter changes consistent with a leukodystrophy. The other sister with hearing loss was well until 34 years of age when she became unsteady on her feet and developed a similar progressive neurological condition and died at the age of 38. Another sister died at 5 years of age from unrelated causes. The proband's other two sisters were healthy with normal hearing at 46 and 50 years. Both parents died in their 60s from cancer. The proband has 3 children all of who are in good health.

Patient 4

The proband is the second child of unrelated Australian parents. His mother had gestational diabetes, but the pregnancy was otherwise uncomplicated. He was born at term, with Apgar scores of 9 and 10 at one and five minutes respectively. Growth was normal, and plagiocephaly in infancy required no surgical intervention. His parents first became concerned about him at five months of age because he could not lift his head when he was in the prone position. Subsequent motor development was delayed: he sat unaided at 8 months, pulled to stand at 12 months, walked unsupported at 18 months. Significant extensor neck weakness persisted in the early years.

Examination at two years of age revealed a normally grown boy with persistence of mild plagiocephaly. He had good muscle bulk and no obvious facial weakness. He had obvious weakness of neck flexion and extension, generalized hypotonia, as well as mild peripheral limb muscle weakness. The Gower manoeuvre was positive. Deep tendon reflexes were normal, and plantars were bilaterally down-going. He was slow and awkward running. Stamina was also poor, precluding him from being able to play sports during childhood.

Trials of a mitochondrial "cocktail" including coenzyme Q10, L-carnitine and riboflavin were associated with subjective improvement in stamina, and a deterioration was noted when the cocktail was stopped.

Over the years his neck and peripheral muscle strength returned to normal, and a structured exercise program was commenced in adolescence, with an improvement in stamina, such that he was able to participate in normal sports.

Cognitive development has been entirely normal, with completion of high school at the age of 17 years. He has never complained of chewing or swallowing difficulties, and formal evaluation over the years demonstrated normal cardiac structure and function, hearing and vision.

His older brother and parents were all healthy with no muscle weakness or other complaints, and there was a great paternal uncle who had had motor neuron disease.

When last reviewed at 17 years of age he had normal muscle bulk, strength and deep tendon reflexes, no myasthenic signs and a negative Gower manoeuvre. His weight was 87.8 kg (93rd percentile) and height was 176.6 cm (53rd percentile).

Biochemical investigations over the years have included blood lactate (2.5 – 3.4 mmol/L; normal range 0.7 – 2.0), CPK (220 – 240 IU/L; normal range 15 – 180), and liver enzymes and renal function testing (always normal).

A neck muscle biopsy at the age of two years showed marked variation in muscle fiber size with many small degenerate fibers and some regenerating fibers (Figure 1a). There was a mild increase in the number of central nuclei, and mild peri-and endomysial fibrosis was seen. There was evidence of an unusual form of degeneration, with the Gomori trichome stain showing a flocculent grey granular appearance and accumulation of mitochondria, whilst the acid phosphatase stain also showed changes consistent with degeneration. Fiber typing showed a marked reduction of Type I fibers. Oil Red O staining revealed increased large droplets, many of which had irregular shapes.

A quadriceps muscle biopsy taken at the same time showed mild variation of muscle fiber size, probably within normal limits (Figure 1a). There was no increase in central nuclei, but the Gomori trichome staining revealed subsarcolemmal accumulation of mitochondria, with other stains normal and indicative of a normal fiber type distribution.

Electron microscopy of neck muscle biopsy showed changes suggestive of a mitochondrial myopathy. There were frequent large subsarcolemmal aggregates of enlarged pleomorphic mitochondria with abnormal cristae and large electron dense bodies. Giant mitochondria were also seen. Electron microscopy of quadriceps muscle was normal.

Muscle respiratory chain enzymology revealed an isolated low complex I activity (35%, 49% and 16% of control mean relative to protein, citrate synthase and complex II respectively), whilst fibroblast respiratory chain enzyme activities were normal.³⁴

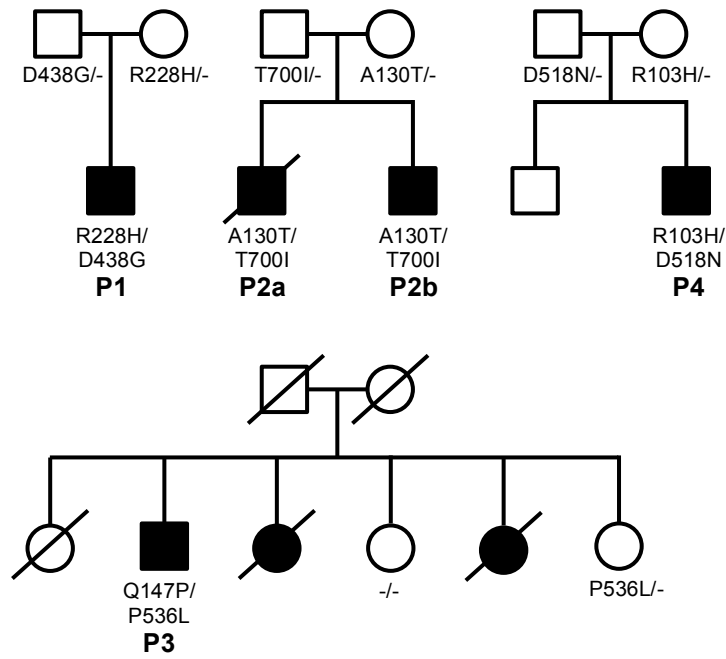


Figure S1. Family pedigrees showing inheritance of *LARS2* missense variants

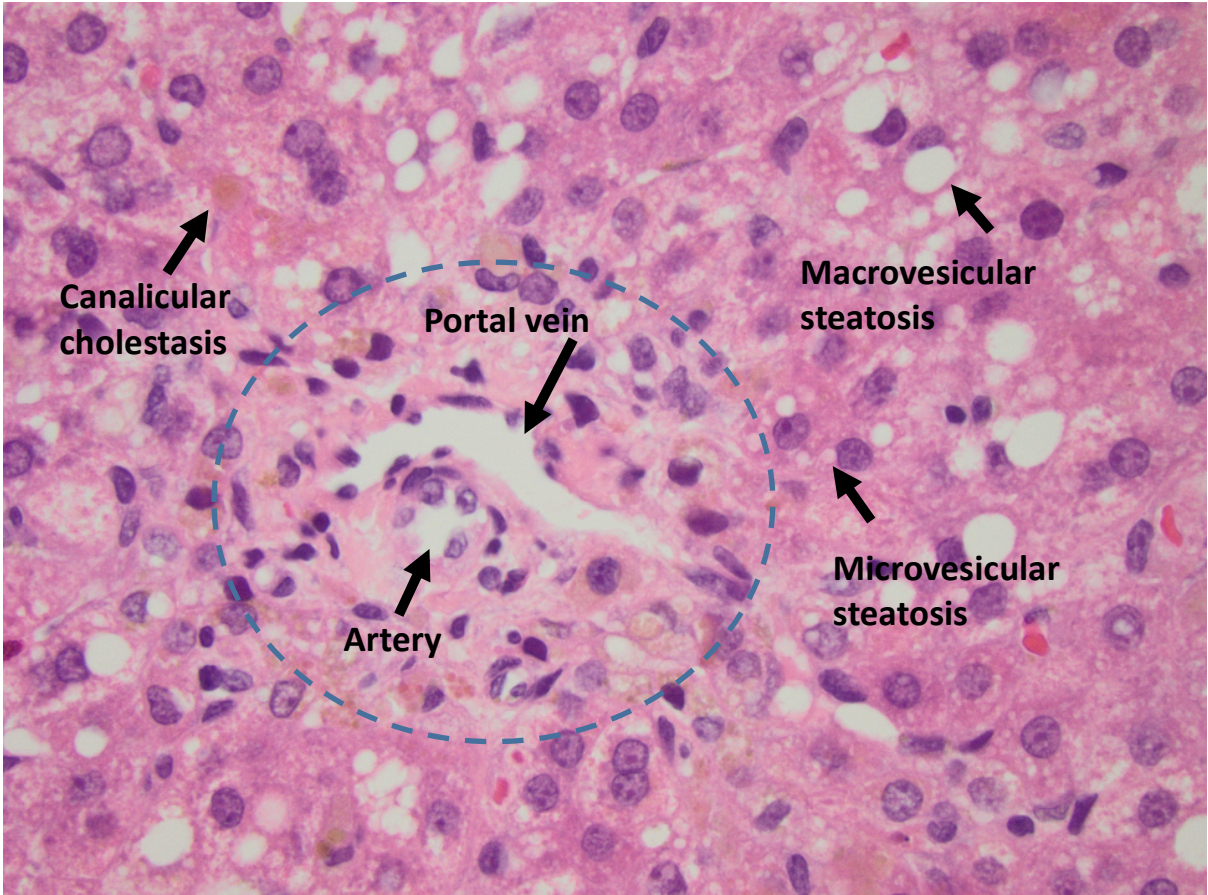


Figure S2. Liver biopsy of Patient 1. Haematoxylin and eosin staining showing portal tract without bile duct, cholestasis, mixed macrovesicular and microvesicular steatosis.

<i>LARS2 Arg103His</i>	93	PSGKLHMGHVHVYTISDTIA
<i>H. sapiens</i>	93	PSGKLHMGHVRVYTISDTIA
<i>B. taurus</i>	93	PSGKLHMGHVRVYTISDTIA
<i>M. musculus</i>	92	PSGKLHMGHVRVYTISDTIA
<i>G. gallus</i>	100	PSGKLHMGHVRVYTISDTIA
<i>X. laevis</i>	89	PSGKLHMGHVRVYTISDTIA
<i>D. rerio</i>	80	PSGRLHMGHVRVYAIISDTIS
<i>C. elegans</i>	68	PSGRLHIGHMRVYTISDATA
<i>S. cerevisiae</i>	58	PSGALHIGHLRVYVISDSL N
<i>E. coli</i>	44	PSGRLHMGHVRNYTIGDVIA
<i>T. thermophilus</i>	44	PSGDLHMGHLKNYTMGDVLA

<i>LARS2 Ala130Thr</i>	120	MQVINPMGWDTFGLPAENAA
<i>H. sapiens</i>	120	MQVINPMGWDAFGLPAENAA
<i>B. taurus</i>	120	MQVINPMGWDAFGLPAENAA
<i>M. musculus</i>	119	MQVINPMGWDAFGLPAENAA
<i>G. gallus</i>	127	MQVLNPMGWDAFGLPAENAA
<i>X. laevis</i>	116	MQVINPMGWDAFGLPAENAA
<i>D. rerio</i>	107	HQVLNPMGWDAFGLPAENAA
<i>C. elegans</i>	95	YEVIHPIGWDSFGLPAENAA
<i>S. cerevisiae</i>	85	YNVIHPMGWDAFGLPAENAA
<i>E. coli</i>	71	KNVLQPIGWDAFGLPAEGAA
<i>T. thermophilus</i>	71	YEVLHPMGWDAFGLPAENAA

<i>LARS2 Gln147Pro</i>	137	NAAVERN LHPPSWTQSNIKH
<i>H. sapiens</i>	137	NAAVERN LH PQSWTQSNIKH
<i>B. taurus</i>	137	NAAIERN LH PESWTQSNIRH
<i>M. musculus</i>	136	NAAIERN LH PESWTQSNIKH
<i>G. gallus</i>	144	NAAIEHGLHPASWTQSNIQH
<i>X. laevis</i>	133	NAAIEHGLRPDTWTERNIKH
<i>D. rerio</i>	124	NAAIERN LDPEDWTRSNIES
<i>C. elegans</i>	112	NAARDKGVDPREWTINNIES
<i>S. cerevisiae</i>	102	NAAIERSINPAIWTRDNI AK
<i>E. coli</i>	88	GAAVKNN TAPAPWTYDNIAY
<i>T. thermophilus</i>	88	NAALKFGVHPKDWTYANIRQ

<i>LARS2 Arg228His</i>	218	EQVDEHGCSWHS G-AKVEQK
<i>H. sapiens</i>	218	EQVDEHGCSWRS G-AKVEQK
<i>B. taurus</i>	218	EQVDEHGCSWRS G-AKVEQK
<i>M. musculus</i>	217	EQVNEYGCSWRS G-AKVEKK
<i>G. gallus</i>	225	EQVDDNGCSWRS G-AKVEQK
<i>X. laevis</i>	214	EQVDENGCSWRS G-AKVEQK
<i>D. rerio</i>	205	EQVDENGCSWRS G-APVEQK
<i>C. elegans</i>	193	EQIDNDGKSWRS G-AKAEKK
<i>S. cerevisiae</i>	183	EQVDAQGRSWRS G-AIVEKK
<i>E. coli</i>	169	EQVI-DGCCWRCD-TKVERK
<i>T. thermophilus</i>	169	EQVV-EGRCWRHEDTPVEKR

<i>LARS2 Asp438Gly</i>	428	QKARGKRVGGVTSDKLKDW
<i>H. sapiens</i>	428	QKARGKRVGGDVTSDKLDKDW
<i>B. taurus</i>	428	QKARRERVGGDVTSDKLDKDW
<i>M. musculus</i>	427	RKARGMRVGGHVTSNKLKDW
<i>G. gallus</i>	435	QQAKNKGIGGDLMSDKLRDW
<i>X. laevis</i>	424	QQASSEGVGGHLTSDKLRDW
<i>D. rerio</i>	415	QKARQMNVGGHLTSAKLRDW
<i>C. elegans</i>	372	EMASFGGYGGYETSRTLTDW
<i>S. cerevisiae</i>	426	GMLNSEGLSKSVVRYKIRDW
<i>E. coli</i>	401	DKLTAMGVGERKVNYRLRDW
<i>T. thermophilus</i>	403	AWLEEKGLGKGRVITYRLRDW

<i>LARS2 Asp518Asn</i>	508	RCKGAAKRETNTMDTFVDSA
<i>H. sapiens</i>	508	RCKGAAKRETDMDTFVDSA
<i>B. taurus</i>	508	RCKGAATRETDMDTFVDSA
<i>M. musculus</i>	507	RCKGSAKRETDMDTFVDSA
<i>G. gallus</i>	515	RCKAEARREIDTMDTFVDSA
<i>X. laevis</i>	504	RCAGAAVRETDMDTFVDSA
<i>D. rerio</i>	495	RCKGPAERETDMDTFVDSS
<i>C. elegans</i>	436	RFGESGVFDTDLDTFFDSA
<i>S. cerevisiae</i>	505	SCGSPAKRETDMDTFIDSS
<i>E. coli</i>	478	VNGMPALRETDFTDFMESS
<i>T. thermophilus</i>	486	KCGGPAKRDTDMDTFDSS

<i>LARS2 Pro536Leu</i>	526	SAWYYFRYTDLHNPSPFNT
<i>H. sapiens</i>	526	SAWYYFRYTDPHNPSPFNT
<i>B. taurus</i>	526	SAWYYFRYTDPQNTQSPFSA
<i>M. musculus</i>	525	SAWYYFRYTDPHNTQSPFGS
<i>G. gallus</i>	533	SAWYYLRYTDPHNTDRPFNC
<i>X. laevis</i>	522	SAWYYLRYTDPINSEKPFDK
<i>D. rerio</i>	513	SSWYYFRYTDPQNPLRPFER
<i>C. elegans</i>	454	SAWYYLRYLDNKNKSELIS-
<i>S. cerevisiae</i>	523	SSWYYFRFLDPKNTSKPFDR
<i>E. coli</i>	496	SSWYYARYTCPQYKEGMLDS
<i>T. thermophilus</i>	504	SSWYYLRYTDPHNDRLPFDP

<i>LARS2 Thr700Ile</i>	690	RWQQRLWTLTIRFIEAR---
<i>H. sapiens</i>	690	RWQQRLWTLTTRFIEAR---
<i>B. taurus</i>	690	RWQQRLWALVTRFIEAR---
<i>M. musculus</i>	689	RWQQRLWSLTTRFIEAR---
<i>G. gallus</i>	698	RWQTRLWTLVTKLIEAR---
<i>X. laevis</i>	687	RWQTRLWTITSKFIEAR---
<i>D. rerio</i>	678	RWQSRLWGLVSKLRSVR---
<i>C. elegans</i>	617	KLLDRIAAINSQIVDARDN-
<i>S. cerevisiae</i>	695	RWLQKVLHLTKNILSLEKDL
<i>E. coli</i>	668	RFLKRVWKLVEHTAK----
<i>T. thermophilus</i>	686	RFLNRIYRRVAEDREA----

Figure S3. Sequence alignments for LARS2 and homologs showing the location of the LARS2 variants (shaded) and their conservation among selected species.

Table S1. Kinetic parameters for leucylation of *E. coli* tRNA_{5^{Leu}}(UAA) transcript by LARS2 wild-type and variant recombinant proteins. Values are mean (SEM), n ≥ 2.

Patient	LARS2 Variants (NM_015340.3)	K_m (μM)	k_{cat} (min^{-1})	k_{cat}/K_m ($\text{min}^{-1} \mu\text{M}^{-1}$)	Loss in catalytic efficiency[†]
-	WT	1.3 (0.1)	25.8 (4.2)	19.2 (3.0)	1
1	Arg228His	1.7 (0.2)	0.6 (0.0)	0.4 (0.0)	48.0
1	Asp438Gly	0.8 (0.2)	8.5 (0.2)	10.3 (2.0)	1.8
2a, 2b	Ala130Thr	1.8 (0.6)	2.2 (0.6)	1.2 (0.1)	16.0
2a, 2b	Thr700Ile	1.1 (0.1)	7.7 (0.6)	7.1 (0.3)	2.7
3	Gln147Pro	1.6 (0.1)	13.5 (1.8)	8.7 (1.4)	2.2
3	Pro536Leu	0.9 (0.1)	2.9 (0.8)	3.1 (0.9)	6.2
4	Arg103His	0.3 (0.1)	3.0 (0.3)	11.9 (1.1)	1.6
4	Asp518Asn	2.2 (0.5)	7.2 (1.9)	3.3 (0.6)	5.8

[†]Loss of efficiency is calculated as a fold-change relative to wild-type (WT) LARS2

